Fundamental limits in fiber Bragg grating peak wavelength measurements*

Shellee D. Dyer‡, Paul A. Williams, R. Joseph Espejo,
Jonathan D. Kofler, and Shelley M. Etzel
National Institute of Standards and Technology, Optoelectronics Division
325 Broadway, Boulder, CO 80305 USA

ABSTRACT

We discuss the fundamental limits of fiber Bragg grating (FBG) wavelength metrology. High-accuracy wavelength measurements are critical for FBG strain sensors because a wavelength measurement uncertainty as small as 1 pm leads to an uncertainty of nearly 1 microstrain. We compare the measurement uncertainties for several common wavelength-measurement systems, including tunable laser, optical spectrum analyzer (OSA), and interferometric. We show that when using an OSA it is difficult to achieve a measurement uncertainty better than 10 pm, and if the OSA is not accurately calibrated to a known wavelength reference, then the wavelength measurement uncertainty can be as large as 1 nm. We describe the uncertainties involved in determining peak and/or centroid wavelength from a measured data set. We also discuss calibration references for FBG sensor interrogation units. Wavelength references that are based on molecular absorption lines are often an excellent choice for FBG sensor calibration. However, some interrogation units require a wavelength reference unit based on narrow reflection lines rather than absorption lines. We investigated the application of athermally packaged FBGs as wavelength references, but we found that their wavelengths will drift with time and can undergo large jumps. We concluded that it is difficult to achieve stability better than 4 pm/year in athermally packaged FBGs.
Keywords: calibration; fiber Bragg gratings; fiber-optic sensors; metrology

1. INTRODUCTION

In this paper we discuss the current status of fiber Bragg grating (FBG) metrology, with particular emphasis on important issues for the FBG sensor industry. Some key metrology considerations for FBG-based fiber-optic sensors include high-accuracy measurements of FBG peak or center wavelength, long-term FBG wavelength stability, and calibrations of both the transducer element and the FBG sensor interrogation unit. High-accuracy measurements and calibrations are crucial for FBG-based strain sensors because a wavelength measurement error as small as 1 pm is equivalent to an error of nearly 1 microstrain. Long-term wavelength stability is particularly important in cases where the FBGs are used as wavelength references for calibrating FBG interrogation units. In many applications, molecular absorption lines such as hydrogen cyanide and acetylene are ideal as wavelength reference standards. These molecular absorption lines have been characterized with expanded uncertainty (2σ) as small as 0.1 pm.[1] However, some high-wavelength-accuracy applications are not compatible with absorption-line references. For example, there are some wavelength regions for which there are no appropriate molecular absorption lines. Also, the calibration of some fiber-optic sensor interrogation units may require a wavelength reference based on narrow reflection spectra rather than absorption lines.

We investigated the long-term wavelength stability of several athermally packaged FBGs for wavelength-reference applications, and we determined that the wavelength drift can be quite large. This long-term drift has significant implications for FBG-based sensors because the stability of an athermally packaged FBG is likely determined by drift in the strain applied by the package, particularly in the adhesives that attach the fiber to its package. This packaging drift is an important consideration for FBG-based sensors, where long-term drift in the adhesives of a surface-attached sensor can create large uncertainty in the sensor's measured data.

---

‡ Telephone: 303-497-7463, FAX: 303-497-7621, email: sdyer@boulder.nist.gov

17th International Conference on Optical Fibre Sensors, Marc Voet, Reinhardt Willsch, Wolfgang Ecke, Julian Jones, Brian Culshaw, eds., Proceedings of SPIE Vol. 5855 (SPIE, Bellingham, WA, 2005) · 0277-786X/05/$15 · doi: 10.1117/12.623444

2. FBG MEASUREMENTS

Common FBG measurement systems include tunable laser, interferometric, and optical spectrum analyzer (OSA). We have measured multiple FBGs with each system, compared the results, and quantified the uncertainties of our measurement systems.

2.1 Tunable laser measurement system

Our tunable-laser measurement system is shown in Fig. 1. We use a wavelength meter that is periodically calibrated to a rubidium line to monitor the laser's wavelength. A tunable fiber Fabry-Perot (FFP) filter removes much of the amplified spontaneous emission from the laser output, yielding a higher signal-to-noise ratio (SNR). The SNR is further improved with a chopper and lock-in amplifiers at the detectors. We measure both the laser power and the power reflected by the FBG; we are then able to divide out fluctuations in laser power. For high-accuracy results, it is important to remove these fluctuations in laser power from the measured signal. The uncertainty of this measurement system is determined primarily by the wavelength meter, with standard uncertainty less than 0.1 pm; this does not include the uncertainty of the peak wavelength calculation discussed in Sec 2.4. This measurement, with its low uncertainty, is our primary method for characterizing the long-term stability of our gratings.

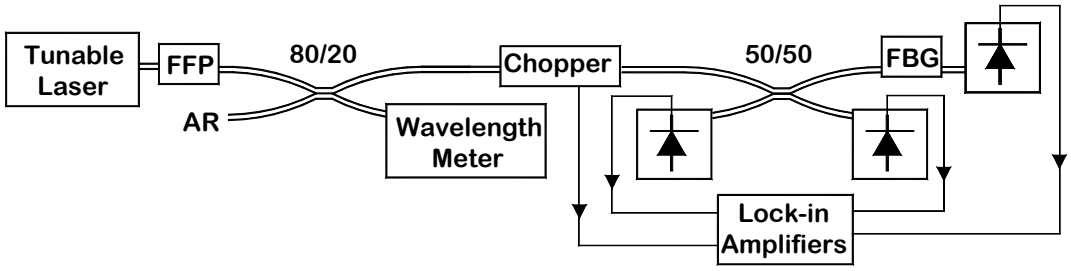

Figure 1. Diagram of tunable-laser measurement system. AR: anti-reflection beam dump, FFP: fiber Fabry-Perot filter.

2.2 Optical spectrum analyzer

OSAs provide a fast and easy measurement of FBG spectra. Unfortunately, an OSA is often a poor choice if high-accuracy results are needed. One source of error is wavelength calibration. This error is often quite large, but it can be measured and corrected using a molecular absorption-line wavelength reference standard.[1] However, after the wavelength calibration error is corrected, the OSA wavelength scale has a nonlinear wavelength uncertainty; we measured 2 pm nonlinearity over a very short wavelength range (2 nm), and some OSA manufacturers specify nonlinearities as large as ± 20 pm over a wavelength range of 40 nm. Another source of error is the wavelength resolution of the OSA; its effect on the measured spectrum is to convolve the FBG spectrum with the OSA's instrument transfer function. If the wavelength resolution is comparable to the width of the FBG reflection spectrum, this convolution can significantly affect the measurement, particularly for the case of an FBG spectrum with strong asymmetry. The effect of OSA wavelength resolution on our FBG measurements was as large as 3 pm for an FBG spectrum that was approximately 100 pm wide and an OSA wavelength resolution of 70 pm. Therefore, an OSA is not appropriate for high-accuracy measurements (< 10-20 pm, depending on the OSA). For measurements that require moderate wavelength accuracy (10-100 pm) the OSA should be used with caution; the OSA must be calibrated periodically to a wavelength reference, and the effects of wavelength resolution and nonlinearity must be included in the assessment of the measurement uncertainty.

2.3 Interferometric measurement system

We have also developed an interferometric system for measuring FBGs, as shown in Fig. 2. This measurement system is a modified version of the system developed by D. Flavin et al.[2] Multiple FBGs written on a single fiber can be measured simultaneously using this system, provided that each FBG has a unique nominal wavelength. The FBGs are illuminated by a broadband source; we used a superfluorescent source with a mean wavelength of approximately 1565 nm and a spectral width of approximately 80 nm. The light reflected from the FBGs is directed into a fiber-optic Mach-Zehnder interferometer. A variable-length air path is included in one arm of the interferometer so that the total optical

path difference (OPD) of the interferometer can be varied. A 1300 nm Nd:YAG laser propagates in the same interferometer to provide a high-coherence interference signal that precisely tracks the OPD. The 1300 nm interference signal is directed onto a photodiode/transimpedance amplifier and then to a zero-crossing circuit. The output of the zero-crossing circuit triggers sampling of the FBG reflection interference signal. From a measured 2^{16} point interferogram, we calculated the centroid wavelength of each grating using Hilbert transforms. We calculated the Hilbert transform by first computing a Fourier transform of our measured data. Then we set all negative frequencies of the spectrum to zero and applied a window (typically 2 nm wide) to the positive frequencies so that only a single FBG spectrum was preserved. We then completed the Hilbert transform calculation by computing an inverse Fourier transform of the windowed signal. Although the Hilbert transform result is discrete, the phrase "analytic signal" is commonly used to describe it. The slope of the phase of the analytic signal is proportional to the grating's centroid wavelength. Fitting a linear curve to the central portion of the phase of the analytic signal gives the centroid wavelength of the FBG. The centroid wavelengths of each FBG in a multiplexed series of gratings can be determined by repeating this calculation process with the spectral window centered upon each of the gratings[2].

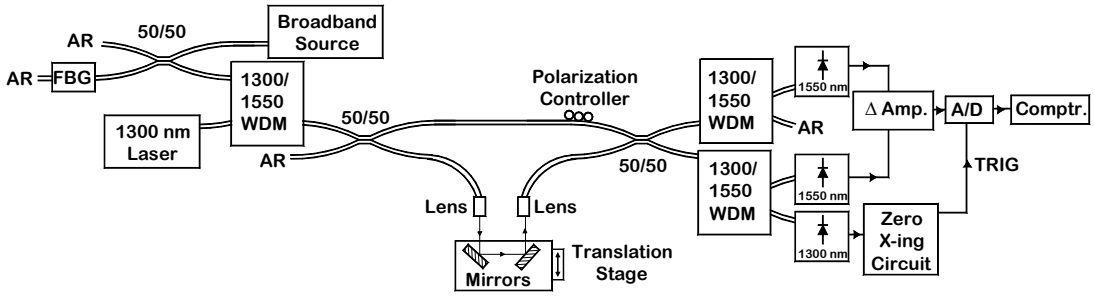

Figure 2. Diagram of an interferometric measurement system for determining FBG wavelengths. Although only one FBG is shown (upper left-hand corner of the diagram), this system can measure multiple FBGs simultaneously. A/D: analog-to-digital card, AR: anti-reflection beam dump, WDM: wavelength-division multiplexing fiber coupler, Δ Amp.: difference amplifier.

2.4 Center, peak, and centroid wavelengths

Measurement techniques such as the tunable-laser and OSA systems measure the FBG's reflectance as a function of wavelength, which leaves the problem of determining the peak, center, or centroid wavelength of the FBG from the measured data. We used a simulation to compare the uncertainties of different methods for identifying the peak and/or centroid location from a measured data set. We created a simulated spectrum assuming a uniform FBG profile and added Gaussian white noise. One way to determine the peak wavelength is use of a maximum-value search of the noisy spectral data. Another is calculation of the centroid wavelength using a 2 nm window of the spectral data as follows:

$$\lambda_c = \frac{\sum_j \lambda_j I_j}{\sum_j I_j}, \tag{1}$$

where λ_j are the measured wavelengths and I_j are the corresponding reflected powers.[3] Another peak wavelength algorithm involved calculating the mean of the wavelengths of the two data points whose reflectance was closest to the half maximum reflectance. We also used curve fits to calculate the peak wavelengths. First, we truncated the measured reflectance data at –1.5 dB below the maximum measured reflectance point. We then fitted a fourth-order polynomial to the central portion of the reflection spectrum and determined the peak wavelength by differentiating the resultant polynomial. We found that the order of the polynomial did not significantly impact the results, unless a very high-order polynomial was used to fit a noisy data set; in that case the polynomial tried to follow the noise. We also fit the truncated data to a Gaussian function. We calculated the uncertainty of these peak wavelength routines from repeated simulations in which the noise was random, but the SNR was held constant. The uncertainty was determined from the

standard deviation of 50 repeated simulations. In Fig. 3a, we compare the uncertainty of these peak wavelength calculation routines. The peak-wavelength search and centroid wavelength calculation are susceptible to noise and work poorly for low SNR, as we expected. The mean of half maxima algorithm gives good results, as shown in Fig. 3a; it seems to be relatively insensitive to noise as a result of the steep slope of the reflection spectrum at the half maxima wavelengths. The mean of half maxima algorithm is relatively easy to implement and is likely a good choice for many applications. The Gaussian and polynomial curve fits also yield good results. It is important to note that the curve fit uncertainty is affected by both the spectral shape and sampling density of a discrete FBG spectrum, as shown in Fig. 3b. The spectral shape of a uniform profile FBG is directly related to its peak reflectance (R_{max}). Strong gratings tend to have flat-topped reflection spectra that are difficult to curve fit, hence the higher uncertainty shown in Fig. 3b. For sensor applications it is best to avoid FBGs with unusual shapes in their reflection spectra and choose FBGs that have narrow reflection spectra with clearly identifiable peaks. Also, if the FBG spectrum is sampled with a dense sampling rate (small $\Delta\lambda$), then the curve fit results are improved, as shown in Fig. 3b.

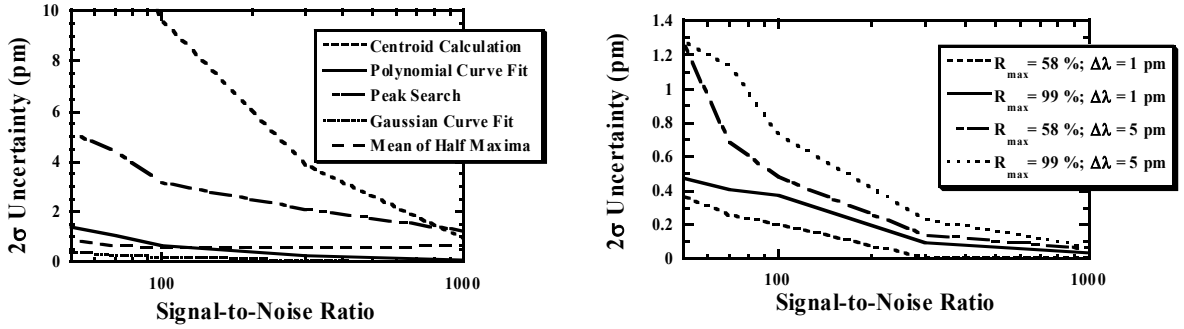

Figure 3. (a) Comparison of the peak/centroid wavelength uncertainty from peak search routine, polynomial and Gaussian curve fits, mean of half maxima, and a centroid calculation assuming a uniform grating with moderate peak reflectance (58 %) and a wavelength sample spacing ($\Delta\lambda$) of 1 pm. (b) Comparison of the effects of grating strength and wavelength sampling density on the peak wavelength uncertainty for a Gaussian curve fit.

2.5 Polarization dependent wavelength shift (PDWS)

Some FBGs exhibit birefringence arising from asymmetric fiber core geometry or the UV writing process. This birefringence results in a polarization dependence of the grating's Bragg wavelength. We measured the PDWS of our gratings used in this paper using a four-polarization state method.[4] All the gratings described in this work have PDWS less than 1 pm.

2.6 Measurement uncertainties and data intercomparison

Our goal was to measure the peak wavelength of FBGs with an uncertainty better than 1 pm. Our tunable-laser measurement described above has an uncertainty of 0.1 pm, but that describes only the wavelength uncertainty of each data point rather than the uncertainty of the peak or center wavelength determined from the measured data. To calculate the uncertainty of the peak wavelength, we combined in quadrature the measurement system uncertainty with the uncertainty of the peak or center wavelength identification routine. For example, the uncertainty of the polynomial curve-fit routine described in section 2.4 is limited primarily by the effects of noise on the reproducibility of the curve fit. This uncertainty is strongly dependent on the shape of the reflection spectrum, as shown in Fig. 3b. Therefore, we quantified this uncertainty for each grating by comparing the results of repeated measurements of that FBG. We calculated the total uncertainty from a quadrature combination of the uncertainties of the measurement system and of the curve fit. The results of the tunable laser measurement and the corresponding uncertainties for four different FBGs are shown in Table 1.

The largest source of uncertainty in the interferometric measurement system is the cosine error that occurs when the reference laser and the measurement signal are not exactly collinear.[5] In the measurement system shown in Fig. 2, we have eliminated this uncertainty by coupling both the measurement signal and the reference laser into the same single-mode fiber. Another source of uncertainty is sampling error; any nonuniformity in the rate at which the signal is sampled will result in a broadening of the spectral function after the signal is Fourier transformed. This spectral broadening can significantly affect the centroid wavelength calculation. We minimized this error by referencing the

sampling rate to the high-coherence interferometric signal from the Nd:YAG laser; in that case this error is limited only by the wavelength stability of the Nd:YAG laser, which is better than 1 pm. The measurement SNR can also affect the centroid wavelength result, but this effect is generally small since the noise is approximately uniformly distributed across the spectrum. Other factors that affect the uncertainty include the interferogram scan length, the size of the spectral window, and the centering of the window with respect to the peak of the spectrum. One advantage of the Hilbert method compared with conventional Fourier transform spectroscopy is that the Hilbert method gives better wavelength resolution for short interferogram lengths.[2,5] For our measurements, we found that a 2^{16} point interferogram, which is equivalent to 43 mm OPD, was sufficient to achieve uncertainty on the order of 1 pm. The size of the spectral window should be chosen to be as large as possible, but if multiple FBGs are measured simultaneously, the maximum window span is limited by how closely spaced the FBGs are. If this measurement is used as an FBG sensor demultiplexer unit, then the window span and FBG wavelength spacing must be wide enough to accommodate the measurand-induced changes in the nominal FBG wavelengths. We used spectral windows with 2 nm width, which allows the FBGs to be closely packed in wavelength, but still allows uncertainty on the order of 1 pm to be achieved. Another factor that limits the uncertainty of the interferometric method is the width of the window applied to the phase of the analytic signal before the linear curve fit is calculated. The phase of the analytic signal as a function of OPD is most linear near its center, where the magnitude of that function is large. Further from the center, the phase rapidly becomes nonlinear. These nonlinearities arise from interference beating between the spectral window and the FBG spectrum. If the spectral window is exactly centered on the FBG spectral peak, then there is no interference beating between the two functions. Unfortunately, that is not practical because the FBG spectrum is discretely sampled, and it is unlikely that a sample occurs exactly at the peak of the spectrum. The spectral window can be centered only on a discrete sample, which typically results in a slight frequency difference between the FBG spectrum and the spectral window, and therefore we have beating between those two functions. The lowest uncertainty is achieved when the linear curve fit is applied to only the central 0.05 % of the analytic signal phase, which allows us to avoid the nonlinearities in that function.

We compared of the wavelengths of four different athermally packaged FBGs measured with both the tunable-laser measurement system and the interferometric system. This comparison was complicated by the fact that the interferometric system determines the centroid wavelength, but for lowest measurement uncertainty in the tunable-laser system, we used the peak rather than the centroid or center wavelengths. For comparison with the interferometric results, we calculated both the peak and the centroid wavelengths of the tunable-laser results.

Our measurement results for four different FBGs are shown in Table 1. One important result is that the difference between the centroid and peak wavelengths of a given FBG can be quite large, especially if the grating is asymmetric. The uncertainties shown in the table were calculated from repeated measurements of each grating. For the tunable laser measurements, the uncertainty of the peak wavelength is smaller than the uncertainty of the centroid wavelength calculation, as discussed in Sec. 2.4. Also, the uncertainties depend on the exact shape of the gratings' reflection spectra, as discussed in Sec. 2.4.

All of our FBGs exhibited wavelength drift, as discussed in Section 3. However, for the results shown in Table 1, we were interested in comparing results from our two different measurement systems to illustrate their low measurement uncertainty. Therefore, the measurements shown in Table 1 were all made within a relatively short period (3 weeks).

Table 1. Comparison of FBG wavelengths measured by tunable laser (TL) and interferometric (I) systems. The numbers in parentheses represent the standard uncertainty (1σ) in the last digit of each measurement. Δ (peak – centroid) compares the peak and centroid wavelengths computed from tunable laser measurements, and Δ (TL – I) compares the centroid results of the two different measurement systems.

Grating	TL (peak) (nm)	TL (centroid) (nm)	I (centroid) (nm)	Δ (peak – centroid) (pm)	Δ (TL–I) (pm)
A	1534.9734 (5)	1534.9790 (12)	1534.9788 (8)	-5.6	0.2
B	1547.4853 (4)	1547.4859 (12)	1547.4861 (7)	-0.6	-0.2
C	1559.9882 (4)	1559.9820 (12)	1559.9826 (6)	6.2	-0.6
D	1574.9930 (3)	1574.9867 (12)	1574.9877 (12)	6.3	-1.0

3. FBG LONG-TERM STABILITY

We investigated the long-term stability of several athermally packaged FBGs from different manufacturers. We found that all of our FBGs had thermal response lower than 0.5 pm/ºC. This was still large enough to potentially affect our stability measurements, so we added an external temperature controller to hold the temperature of the FBGs stable to 0.02 ^{o}C. All of the FBGs that we tested experienced a slow wavelength drift at rates as high as 1 pm over 3 months. We also measured abrupt wavelength jumps as large as 1 nm in more than one FBG. We attribute the wavelength drift to relaxation of strain in the FBG's athermal packaging, while a failure of the adhesives in the athermal package might be responsible for the large and abrupt wavelength jump. We tried exposing the FBGs to many thermal cycles of 0-80 ºC in an attempt to accelerate the aging process and achieve better stability, but with limited success. An example of an FBG stability plot is shown in Fig. 4. The sharp drop in wavelength immediately after the thermal cycle might be attributed to the lack of adequate time for the FBGs to equilibrate after thermal cycling. However, lack of equilibration would be surprising since the measurements were performed at least 20 hours after the last thermal cycle was completed.

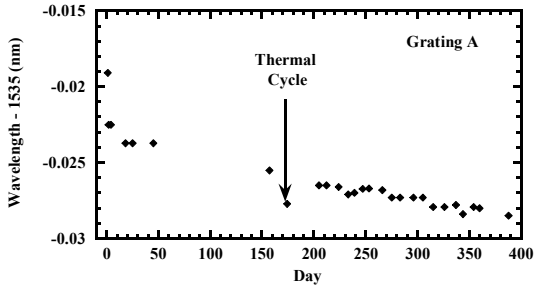

Figure 4. Long-term peak wavelength stability of an athermally packaged FBG with external temperature stabilization.

4. CONCLUSIONS

We have assessed the uncertainty of three common FBG measurement systems. OSA measurements are not appropriate for applications where low uncertainty is desired. High-accuracy measurements, such as the tunable laser or interferometric measurements described above, are preferable. It is important to note that some measurements return the peak wavelength, but others yield the centroid wavelength; for gratings with asymmetric reflection spectra, we found that the peak and centroid wavelengths can differ by as much as 6 pm.

Most packaged FBGs currently lack the stability needed for high-accuracy metrology applications. All of the FBGs that we tested exhibited slow wavelength drifts at rates as high as 1 pm over 3 months. We also measured abrupt wavelength jumps as large as 1 nm in more than one of our FBGs. If these gratings were used to calibrate an FBG strain sensor, this could result in an apparent (but false) strain drift as large as 3 microstrain over a one-year period and the possibility of errors as large as 800 microstrain resulting from adhesive failures in the FBG packaging.

REFERENCES

1. S.L. Gilbert and W. C. Swann, "Standard reference materials: acetylene $^{12}C_2H_2$ absorption reference for 1510 nm to 1540 nm wavelength calibration – SRM 2517a," NIST Spec. Publ. 260-133 (2001 edition).
2. D. A. Flavin, R. McBride, and J. D. C. Jones, "Short scan interrogation and multiplexing of fiber Bragg grating sensors," *Optics Communications*, **170**, pp. 347-353, Nov. 1999.
3. A. Othonos and K. Kalli, *Fiber Bragg Gratings: Fundamentals and Applications in Telecommunications and Sensing*, pp. 318-319, Artech House, Boston, 1999.
4. W. C. Swann, S. D. Dyer and R. M. Craig, "Four state measurement method for polarization dependent wavelength shift," in *Symposium on Optical Fiber Measurements*, Natl. Inst. Stand. Technol. Spec. Publ. 988, pp. 125-128, 2002.
5. K. B. Rochford and S. D. Dyer, "Demultiplexing of interferometrically interrogated fiber Bragg grating sensors using Hilbert transform processing," *J. Lightwave Technol*., **17**, pp. 831- 836, May 1999.